Talanta 85 (2011) 1225–1228

Contents lists available at ScienceDirect

Talanta

journal homepage: www.elsevier.com/locate/talanta

Short communication

Use of 3-D plots to avoid mutual interference in bianalyte ASV determinations: Application to cadmium and lead detection

Nongnoot Wongkaew[a], Cristian Guajardo[b], Patsamon Rijiravanich[c], Mithran Somasundrum[c,*], Werasak Surareungchai[a,b,**]

[a] School of Bioresources and Technology, King Mongkut's University of Technology Thonburi, Bangkhuntien, Bangkok 10150, Thailand
[b] Biological Engineering Graduate Program, King Mongkut's University of Technology Thonburi, Bangkhuntien, Bangkok 10150, Thailand
[c] Biochemical Engineering and Pilot Plant Research and Development Unit, National Center for Genetic Engineering and Biotechnology, King Mongkut's University of Technology Thonburi, Bangkhuntien, Bangkok 10150, Thailand

ARTICLE INFO

Article history:
Received 11 March 2011
Received in revised form 11 May 2011
Accepted 12 May 2011
Available online 19 May 2011

Keywords:
Anodic stripping voltammetry
Cadmium
Lead
Bismuth film
Screen-printed electrode

ABSTRACT

We have examined the anodic stripping voltammetry (ASV) of Cd and Pb at carbon screen printed electrodes modified by an *in situ* deposited Bi film, and have demonstrated significant cross talk between the stripping peaks of the two metals. A simple and generally applicable method for dealing with this problem is described, based on curve-fitting three-dimensional calibration plots using MATLAB. Non-linear fitting to the calibrations produced coefficients of determination $R^2 > 0.99$ for both metals. We have illustrated use of the plots in conjunction with Bi-plated electrodes by measuring 15 randomly selected mixtures of Cd and Pb of known concentration.

1. Introduction

The detection of toxic trace metals is an important analytical application. Current detection methods include atomic absorption spectroscopy, atomic emission spectroscopy, neutron activation analysis and electrochemical methods. Electrochemical measurement is of particular interest due to the fact that it uses relatively inexpensive, often portable equipment and, with anodic stripping voltammetry (ASV), can provide high sensitivities through the preconcentration step in ASV. In practical determinations it will often be the case that more than one metal needs to be measured. For example, the simultaneous determination of Cd and Pb by ASV has been extensively researched [1–30] due to the importance of monitoring Cd and Pb in the environment. The electrode materials for these studies were Hg either in the form of a hanging drop [1–6], a film on glassy carbon [7–10], or on wax-impregnated graphite [11,12], as well as screen printed carbon [13], a solid electrode, or a carbon paste, modified by a chelator or clay [14–19], or by carbon nanotubes [20,21]. Alternatively, Bi coatings [22–26] and Bi bulk electrodes [27] have been used for Cd and Pb analysis, as well as boron-doped diamond [28]. A problem encountered in these determinations is that variations in the concentration of one metal can lead to variations in the response of the other. While this effect has been noted by some researchers [3,19,29], in most ASV determinations of Cd and Pb [1,2,6–15,17,18,20–27,30] it has not been addressed, due to only having Cd and Pb present at equal concentrations, or at a particular fixed ratio. Ensafi et al. [16] and Alipzar et al. [4] have treated the problem by developing artificial neural networks for the data analysis. A simpler approach was suggested by the work of Manivannan et al. [28] who presented the ASV responses of Cd and Pb on 3-D plots. They did not attempt to quantify Cd and Pb at varying concentrations, but suggested quantification would be possible by taking a horizontal cut of the Cd plot at the level of the Cd response, using these concentrations to make a horizontal cut of the Pb plot, and then by going between the two plots successively narrowing down the range of possible Cd and Pb values. This procedure may be extremely time consuming in practice. However, as we demonstrate, 3-D plots can be used to determine Cd and Pb simultaneously by a relatively simple curve-fitting strategy. We illustrate the process with screen printed electrodes bearing *in situ* formed Bi films, as this has shown to be an increasingly used alternative to Hg in ASV [31], due to the high toxicity of Hg and thus practical complications in its use.

---

* Corresponding author.
** Corresponding author at: School of Bioresources and Technology, King Mongkut's University of Technology Thonburi, Bangkhuntien, Bangkok 10150, Thailand.
E-mail addresses: mithran.somasundrum@gmail.com (M. Somasundrum), werasak.sur@kmutt.ac.th (W. Surareungchai).

0039-9140/$ – see front matter © 2011 Elsevier B.V. All rights reserved.
doi:10.1016/j.talanta.2011.05.024

2. Experimental

2.1. Apparatus

Electrochemical experiments were performed using an Autolab PGSTAT12 computer-controlled potentiostat (Eco Chemie) with GPES software. A standard three electrode configuration was employed, comprising of a screen printed carbon electrode (SPCE) as the working electrode, a Ag|AgCl (3 M NaCl) as the reference and a platinum wire as the counter electrode. SPCEs were fabricated exactly as described previously [32] with the exception that in this case the working area exposed was 1.5 mm × 4 mm.

2.2. Reagents

Stock solutions of cadmium nitrate, lead nitrate and bismuth nitrate pentahydrate were purchased from Fluka and diluted as required with 1 M nitric acid for cadmium and lead, or with 5% nitric acid for bismuth. All solutions were prepared with deionized water (Millipore, Milli Q).

2.3. Procedures

ASV determinations were performed at an *in situ* plated bismuth film in the presence of dissolved oxygen. The three electrodes were immersed in an electrochemical cell containing 1.5 mL of 0.2 M acetate buffer, pH 5.6 + 1000 ppb bismuth(III) and a background scan was recorded as follows: a deposition potential of −1.2 V was applied to the SPCE for 210 s under stirring and then, after a 10 s rest period, stripping was performed by square wave voltammetry (SWV) in quiescent solution by scanning the potential from −1.4 V to 0.3 V (step potential = 5 mV, amplitude = 50 mV, and frequency = 50 Hz). Analysis was then performed using a solution of the same buffer and Bi(III) concentration, but containing the required amounts of Cd and Pb. When recording the analyte scan a pretreatment potential of 0.3 V was first applied for 30 s under stirring to ensure removal of any remaining bismuth from the electrode. The deposition potential and SWV quantification were then applied as before. The analyte voltammogram was then background-subtracted. The purpose of background subtraction was to eliminate the effect of Cd and Pb carry-over from one experiment to the next, which sometimes occurred despite washing the cell, reference and counter electrode with deionized water. A fresh SPCE used for each experiment (background + analyte scan) and each concentration was examined in triplicate.

3. Results and discussion

3.1. ASV at bismuth film electrodes

Calibrations of the Cd(II) and Pb(II), in separate, across the range 10–95 ppb gave linear plots (not shown) following the equations: $y = 0.1104x$ ($R^2 = 0.9893$, and $n = 18$) for Cd(II) and $y = 0.1674x$ ($R^2 = 0.9986$, and $n = 18$) for Pb(II). The presence of the Bi film both enhanced the stripping response and resulted in an anodic shift of the oxidation peaks of Cd(0) and Pb(0) by ca. 20 mV, to approx. −0.75 V and −0.54 V respectively (see Supporting Information, Fig. S-1). Similar stripping peak enhancements have been observed for Bi films on carbon nanotubes [26]. The oxidation potentials found here are similar to those for Cd(0) and Pb(0) at Bi-plated carbon nanotubes [26] and at bulk Bi electrodes [27]. The mutual interference of the Cd(II) and PB(II) ASV response is illustrated in Fig. 1. The background subtracted stripping responses to 60 ppb Cd(II) only and 60 ppb Pb(II) only are both less than the responses to the same analytes present in a 60 ppb Cd(II) + 60 ppb Pb(II) mixture. This is different from the result of Manivannan et al. [28] who used a boron-doped diamond electrode for Cd and Pb determination, and reported that the Pb stripping peak increased in the presence of Cd, but that the Cd peak decreased in the presence of Pb. The explanation proposed by the authors was that due to Cd having a more negative standard potential it was deposited on both the underlying electrode (stripped off at the Cd(0) oxidation potential) and as a monolayer on the existing Pb particles (removed at the Pb(0) oxidation potential). We note that in Fig. 1 the oxidation peak widths at half height ($W_{1/2}$) for Cd(0) in the presence and absence of Pb are significantly different, indicating different strengths of adsorption in the two cases [33]. Therefore, we suggest that when Pb is present in the sample reduction of Cd(II) occurs mainly onto the deposited Pb(0) particles, resulting in multilayer Cd coverage. Stripping of Cd thus occurs around the Cd(0) oxidation potential and removes all but a monolayer/sub-monolayer of the Cd coating. Hence, a greater quantity of Pb means a greater surface area for Cd(II) reduction and so a greater current. In contrast, $W_{1/2}$ for Pb(0) oxidation is roughly the same in the absence and presence of Cd, indicating Pb is reduced onto the Bi film in both cases, consistent with Pb possessing the less negative standard potential. A remaining monolayer/sub-monolayer of Cd on the Pb, stripped off at the Pb(0) oxidation potential, would result in the Pb(0) stripping peak increasing with Cd concentration. The difference between this and the Manivannan et al. result suggests a difference in the structure/size of Pb particles when deposited onto a Bi film compared to boron-doped diamond.

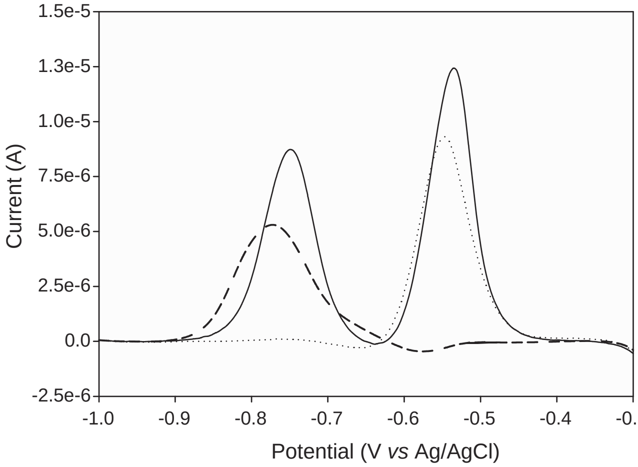

Fig. 1. Background-subtracted square wave (SW) stripping voltammogram at *in situ* deposited Bi film screen printed electrode for 60 ppb Cd^{2+} (- - -), 60 ppb Pb^{2+} (. . .) and 60 ppb Cd^{2+} + 60 ppb Pb^{2+} (—). Electrolyte = 0.2 M acetate buffer, pH 5.6. Deposition potential = −1.2 V, deposition time = 210 s. SW conditions: step potential = 5 mV, amplitude = 50 mV, and frequency = 50 Hz.

3.2. 3-D curve-fitting of ASV data

To generate data for 3-D plots we calibrated Cd and Pb using mixtures in which the concentrations of the ions were varied independently from 0 ppb to 100 ppb in 20 ppb steps, i.e., 36 different Cd:Pb ratios in total. Three electrodes were used for each ratio. Some examples of the stripping square wave voltammograms are given in Supporting Information, Fig. S-2. To match the predicted current for species E, $\hat{i}_E$, to the actual current for E, i_E, at any point on these plots we consider that $\hat{i}_E$ can be described by a polynomial equation composed of j monomials, i.e.,

$$\hat{i}_E = \sum_{j=1}^{n} k_j^E m_j(c, p) \qquad (1)$$

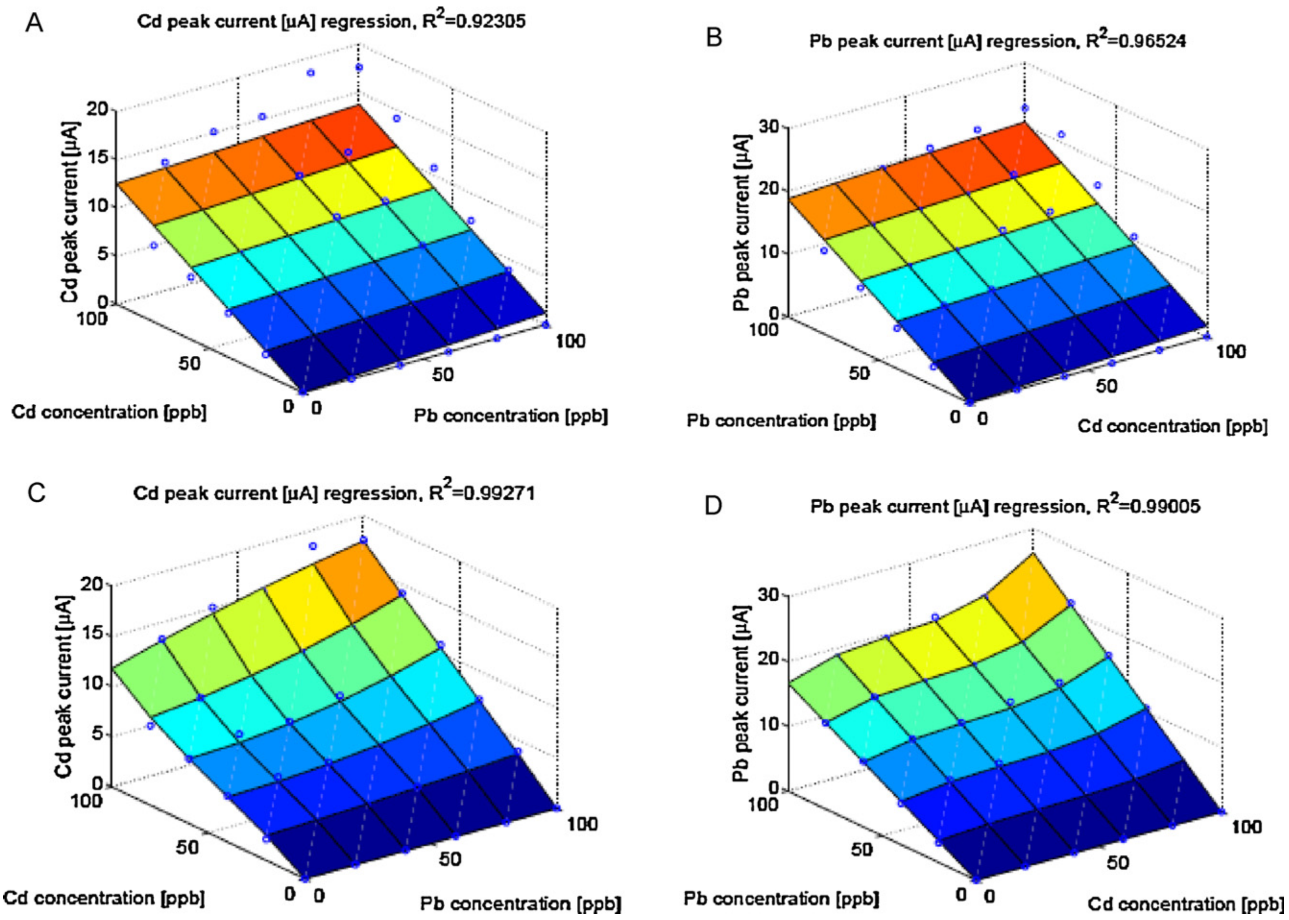

Fig. 2. Three dimensional calibration curves for Cd (A and C) and Pb (B and D). Stripping responses were measured at each intersection on the concentration grid and are shown as circles. Surfaces are plotted using Eqs. (3) and (4) (A and B) or Eqs. (7) and (8) (C and D). Where circles are not visible they are below the plane of the fitting surface.

where k_j^E is the coefficient of the monomial m_j and c and p are the concentrations of Cd and Pb respectively. The values of the coefficients for each m_j are determined by fitting the experimental values of i_E to the particular polynomial for $\hat{i}_E$ using the MATLAB command robustfit. The coefficient of determination, R^2, for the fit is determined from the definition [34]:

$$R^2 = 1 - \frac{\sum_{j=1}^{n} [i_{E_j} - \hat{i}_{E_j}]^2}{\sum_{j=1}^{n} [i_{E_j} - \mathrm{mean}(i_E)]^2} \tag{2}$$

The simplest treatment of the data is achieved by fitting it to a plane for both the Cd and Pb plots. In this case the predicted currents for Cd and Pb will be described by:

$$\hat{i}_p = k_1^p c + k_2^p p \tag{3}$$

$$\hat{i}_c = k_1^c p + k_2^c c \tag{4}$$

from which robustfit gives $k_1^p = 1.73 \times 10^{-2}$, $k_2^p = 1.88 \times 10^{-1}$ ($R^2 = 0.9652$), and $k_1^c = 1.22 \times 10^{-2}$, $k_2^c = 1.25 \times 10^{-1}$ ($R^2 = 0.9231$). As can be seen in Fig. 2A and B, this model has some significant differences from the experimental Cd and Pb currents. Therefore non-linear dependencies of $\hat{i}_E$ were examined. We observed that the value of i_p could be approximated to a cubic function of Cd concentration (see Supporting Information, Fig. S-3A) and hence:

$$\hat{i}_p = a_0 + a_1 c + a_2 c^2 + a_3 c^3 \tag{5}$$

where the coefficients a_j are dependent on the Pb concentration. At a fixed concentration of Cd i_p could be approximated to a linear function of Pb concentration (see Supporting Information, Fig. S-3B), i.e.,

$$\hat{i}_p = b_1 p \tag{6}$$

Combining Eqs. (5) and (6):

$$\hat{i}_p = k_1^p p + k_2^p cp + k_3^p c^2 p + k_4^p c^3 p \tag{7}$$

which in robustfit gives $k_1^p = 1.669 \times 10^{-1}$, $k_2^p = 1.796 \times 10^{-3}$, $k_3^p = -3.938 \times 10^{-5}$, $k_4^p = 3.101 \times 10^{-7}$, $R^2 = 0.9901$. Similarly, for a given concentration of Cd, i_c could be approximated to a quadratic function of Pb concentration, and for a fixed concentration of Pb i_c could be approximated to a cubic function of Cd concentration (see Supporting Information, Fig. S-3C and D). Hence, combining the relations in the same manner as before we have:

$$\begin{aligned} \hat{i}_c &= (a_0 + a_1 p + a_2 p^2)(b_1 c + b_2 c^2 + b_3 c^3) \\ &= k_1^c c + k_2^c pc + k_3^c p^2 c + k_4^c c^2 + k_5^c pc^2 + k_6^c p^2 c^2 + k_7^c c^3 \\ &\quad + k_8^c pc^3 + k_9^c p^2 c^3 \end{aligned} \tag{8}$$

Application of robustfit as before gives $k_1^c = 1.4151 \times 10^{-1}$, $k_2^c = 7.7503 \times 10^{-4}$, $k_3^c = -3.4485 \times 10^{-6}$, $k_4^c = -1.0489 \times 10^{-3}$, $k_5^c = -3.0162 \times 10^{-5}$, $k_6^c = 3.8163 \times 10^{-7}$, $k_7^c = 8.1394 \times 10^{-6}$, $k_8^c = 2.9732 \times 10^{-7}$, $k_9^c = -3.6336 \times 10^{-9}$, $R^2 = 0.9927$. Hence, the correlation is again better than using the linear fit. Taking the above listed values of k_j the *in situ* plated Bi electrodes were validated using a set of 15 known mixtures of Cd(II) and Pb(II) at random combinations, with the concentrations of Cd and Pb determined by fitting to both the linear and non-linear equations. The results are shown in Table 1. As would be expected from the values

Table 1
Validation of Bi-plated electrodes for simultaneous Cd and Pb detrmination by three dimensional calibration. σ_n = standard deviation ($n = 3$).

Real concentration x_i		Mean I Cd (μA)	σ_n	Mean I Pb (μA)	σ_n	Concentration from plane 3D model[a] $\hat{x}_i$		Concentration from polynomial 3D model[b] $\hat{x}_1$		% Mean relative prediction error[c] (real vs. plane 3D model)		% Mean relative prediction error[c] (real vs. polynomial 3D)	
[Cd] (ppb)	[Pb] (ppb)					[Cd] (ppb)	[Pb] (ppb)	[Cd] (ppb)	[Pb] (ppb)	[Cd]	[Pb]	[Cd]	[Pb]
10	10	0.651133	0.14172	1.489667	0.04583	4.48	8	4.61	8.54	−55	−25	−54	−14
10	50	1.655333	0.303767	10.38167	2.627833	7.93	55.7	10.33	57.18	−21	9	3	14
10	90	1.789667	0.454754	18.02333	0.929157	5.01	96.68	9.83	99.56	−50	6	−2	11
17	65	2.769	0.982518	12.98	1.195282	15.56	69.65	17.39	69.11	−8	4	2	7
33	12	2.969	0.817058	2.669333	0.48096	22.57	14.36	23.74	13.94	−32	10	−27	16
46	93	8.519667	1.213808	19.64333	0.20306	58.49	105.48	48.44	99.85	27	6	5	7
50	10	5.331	0.596888	2.289667	1.163345	41.84	12.37	48.06	11.64	−16	−17	−4	16
50	50	6.430333	1.139861	10.16967	3.405601	46.59	54.64	50.52	51.59	−7	−0.4	−1	3
50	90	8.63	1.825591	19.97333	2.162183	59.21	107.25	48.46	101.53	18	12	−4	13
58	47	7.521667	0.757031	9.953	0.688787	55.51	53.5	59.96	49.8	−4	2	3	6
74	72	12.17267	2.539299	17.64333	2.563208	89.03	94.82	77.64	82.42	20	19	5	12
90	10	11.43433	1.700319	1.845	0.589997	91.34	10.09	95.33	7.41	15	−86	5	−27
90	50	12.53333	0.532572	11.652	1.490252	95.08	62.7	89.74	49.57	6	6	−0.3	−1
90	90	15.23667	1.225411	19.66	1.412692	112.71	105.69	93.88	80.25	25	5	4	−11
95	63	15.01333	2.302614	15.04667	2.061973	113.32	80.94	98	58.65	19	10	3	−8

[a] Using Eqs. (3) and (4).

[b] Using Eqs. (7) and (8).

[c] Defined as $\frac{\left((1/n)\sum_{i=1}^{n}\hat{x}_i\right)-x_i}{x_i} \times 100\%$.

of R^2, the non-linear curve-fitting gave a better agreement to the real Cd and Pb concentrations. Obviously, for this particular electrode treatment, improvement of the reproducibility of the screen printed electrode surface would improve the measurement further.

We believe the procedure described here should be generally applicable to bi-analyte mutual interference, since the only requirement of the curve fitting is to approximate each concentration dependence of the 3-D plot to an appropriate mathematical function.

Acknowledgements

Nongnoot Wongkaew acknowledges a Ph.D. scholarship from the Royal Golden Jubilee Project of the Thailand Research Fund. The screen printed electrodes were fabricated by Ms. Kritsanaporn Cheurungsikul at PDTI. This project received financial support from the National Research University Project of Thailand's Office of the Higher Education Commission.

Appendix A. Supplementary data

Supplementary data associated with this article can be found, in the online version, at doi:10.1016/j.talanta.2011.05.024.

References

[1] M.C.V. Mamani, L.M. Aleixo, M.F. de Abreu, S. Rath, J. Pharm. Biomed. Anal. 37 (2005) 709.
[2] M. Panigati, M. Piccone, G. D'alfonso, M. Orioli, M. Carini, Talanta 58 (2002) 481.
[3] C. Locatelli, G. Torsi, Talanta 50 (1999) 1079.
[4] J. Alpizar, A. Cladera, V. Cerda, E. Lastres, L. Garcia, M. Catasus, Anal. Chim. Acta 340 (1997) 149.
[5] J. Opydo, Anal. Chim. Acta 298 (1994) 99.
[6] S.S. Dhaktode, Anal. Chim. Acta 199 (1987) 181.
[7] S. Suteerapataranon, J. Jakmunee, Y. Vaneesorn, K. Grudpan, Talanta 58 (2002) 1235.
[8] D. Jagner, E. Sahlin, L. Renman, Talanta 41 (1994) 515.
[9] D. Jagner, M. Josefson, S. Westerlund, Anal. Chim. Acta 128 (1981) 155.
[10] J. Wang, M. Ariel, Anal. Chim. Acta 101 (1978) 1.
[11] B.S. Sherigara, Y. Shivaraj, R.J. Mascarenhas, A.K. Satpati, Electrochim. Acta 52 (2007) 3137.
[12] S.T. Crosmun, J.A. Dean, J.R. Stockely, Anal. Chim. Acta 75 (1975) 421.
[13] R. Guell, G. Aragay, C. Fintas, E. Antico, A. Merkoci, Anal. Chim. Acta 627 (2008) 219.
[14] Y. Li, X. Liu, X. Zeng, Y. Liu, X. Liu, W. Wei, S. Luo, Sens. Actuators B 139 (2009) 604.
[15] H. Zheng, Z. Yan, H. Dong, B. Ye, Sens. Actuators B 120 (2007) 603.
[16] A.A. Ensafi, T. Khayamian, A. Benvidi, E. Mirmomtaz, Anal. Chim. Acta 561 (2006) 225.
[17] S. Yuan, W. Chen, S. Hu, Talanta 64 (2004) 922.
[18] C. Hu, K. Wu, X. Dai, S. Hu, Talanta 60 (2003) 17.
[19] R. Agraz, M.T. Sevilla, L. Hernandez, Anal. Chim. Acta 273 (1993) 205.
[20] C.R.T. Tarley, V.S. Santos, B.E.L. Baeta, A.C. Pereira, L.T. Kubota, J. Hazard. Mater. 169 (2009) 256.
[21] K. Wu, S. Hu, J. Fei, W. Bai, Anal. Chim. Acta 489 (2003) 215.
[22] D. Li, J. Jia, J. Wang, Talanta 83 (2010) 332.
[23] L. Luo, X. Wang, Y. Ding, Q. Li, J. Jia, D. Deng, App. Clay Sci. 50 (2010) 154.
[24] U.A. Kirgoz, S. Marin, M. Pumera, A. Merkoci, S. Alegret, Electroanalysis 17 (2005) 881.
[25] H. Xu, L. Zeng, D. Huang, Y. Xian, L. Jiu, Food Chem. 109 (2008) 834.
[26] G.H. Hwang, W.K. Han, J.S. Park, S.G. Kang, Talanta 76 (2008) 301.
[27] K.C. Armstrong, C.E. Tatum, R.N. Dansby-Sparks, J.Q. Chambers, Z.-L. Xue, Talanta 82 (2010) 675.
[28] A. Manivannan, R. Kawasaki, D.A. Tryk, A. Fujishima, Electrochim. Acta 49 (2004) 3313.
[29] J.F. van Staden, M.C. Matoetoe, Anal. Chim. Acta 411 (2000) 201.
[30] E. Munoz, S. Palmero, M.A. Garcia-Garcia, Talanta 57 (2002) 985.
[31] A. Economou, Trends Anal. Chem. 24 (2005) 334.
[32] S. Pinijsuwan, P. Rijiravanich, M. Somasundrum, W. Surareungchai, Anal. Chem. 80 (2008) 6779.
[33] K.C. Honeychurch, J.P. Hart, D.C. Cowell, Electroanalysis 12 (2000) 171.
[34] J. Czerminski, A. Iwasiewicz, Z. Paszek, A. Sikorski, Statistical Methods in Applied Chemistry, Elsevier, Amsterdam, 1990, p. 306.